

1 **Impacts of using state-of-the-art multivariate bias correction**
2 **methods on hydrological modeling over North America**

3 Qiang Guo^{1,2}, Jie Chen^{1,2*}, Xunchang John Zhang³, Chong-Yu Xu^{1,4}, Hua Chen¹

4 ¹ State Key Laboratory of Water Resources and Hydropower Engineering Science,
5 Wuhan University, Wuhan 430072, Hubei, P. R. China

6 ² Hubei Provincial Key Lab of Water System Science for Sponge City Construction,
7 Wuhan University, Wuhan 430072, Hubei, P. R. China

8 ³ USDA-ARS Grazinglands Research Lab., 7207 West Cheyenne St., El Reno, OK
9 73036, USA

10 ⁴ Department of Geosciences, University of Oslo, P. O. Box 1047, Blindern, Oslo
11 N-0316, Norway

12 *corresponding author, Email: jiechen@whu.edu.cn; Phone: +86-17764063119

13 **Key points:**

- 14 ● The correction of modeled precipitation-temperature correlations can improve the
15 accuracy of hydrological simulations
- 16 ● The advantages of using multivariate bias correction methods in hydrological
17 simulations are weakened when comes to the validation period
- 18 ● The benefits of correcting precipitation-temperature correlations in hydrological
19 simulations are climate regime-dependent

20 **Abstract:** Bias correction techniques are widely used to bridge the gap between

21 climate model outputs and input requirements of hydrological models to assess the
22 climate change impacts on hydrology. In addition to univariate bias correction
23 methods, several multivariate bias correction methods were proposed recently, which
24 can not only correct the biases in marginal distributions of individual climate
25 variables, but also properly adjust the biased inter-variable correlations simulated by
26 climate models. Due to the diversities of climate regime and climate model bias,
27 hydrological simulation for watersheds under different climate conditions may show
28 various sensitivities to the correction of inter-variable correlations. Therefore, it is of
29 great importance to investigate 1) whether the correction of inter-variable correlations
30 has impacts on the hydrological modeling, and 2) how these impacts vary with
31 watersheds under different climate conditions. To achieve these goals, this study
32 evaluates behaviors and their spatial variability of multiple state-of-the-art
33 multivariate bias correction methods in hydrological modeling over 2840 watersheds
34 distributed in different climate regimes in North America. The results show that,
35 compared to using a quantile mapping univariate bias correction method, applying
36 multivariate methods can improve the simulation of snow proportion, snowmelt,
37 evaporation, and several streamflow variables. In addition, this improvement is more
38 clear for watersheds with arid and warm temperate climates in southern regions, while
39 is limited for northern snow-characterized watersheds. Overall, this study
40 demonstrates the importance of using multivariate bias correction methods instead of
41 univariate methods in hydrological climate change impact studies, especially for

42 watersheds with arid and warm temperate climates.

43 **Keywords:** Multivariate bias correction methods, Hydrological modeling,

44 Inter-variable correlation, Climate regimes, North America

45 **1. INTRODUCTION**

46 Global climate models (GCMs) and regional climate models (RCMs) are useful
47 tools to provide climate change information for future climate change impact studies.

48 However, due to the systematic biases in the climate model simulations, the GCM and

49 RCM outputs are usually not directly applicable to environment models for impact

50 studies (Hakala et al., 2018; Maraun, 2016). Bias correction methods, as a

51 post-processing approach for RCM and GCM outputs, have been widely used in

52 climate change impact studies for several years (Chen et al., 2013a; Li et al., 2019;

53 Shen et al., 2018; Shrestha et al., 2019). Climate model bias can be reflected in

54 several aspects, such as marginal distribution, and inter-variable correlations (Kumar

55 et al., 2014; Mehran et al., 2014). The widely used quantile mapping methods are able

56 to reduce the biases in marginal distribution (Cannon et al., 2015; Gutiérrez et al.,

57 2019) and consistently perform better than other methods (Chen et al., 2013b). Those

58 methods have become standard procedures for using climate model simulations for

59 hydrological impact studies (Chen et al., 2018; Hakala et al., 2018). However, most of

60 those quantile mapping-based methods operate on each climate variable

61 independently without taking biases of inter-variable correlations into consideration.

62 The interdependence of key climate variables, such as precipitation (P) and
63 temperature (T) dependence, may be crucial for modeling hydrological processes in
64 impact studies. For example, the P-T correlation can influence the transition between
65 rainfall and snowfall, and also the snowmelt process (Chen et al., 2018; Meyer et al.,
66 2019). With further development of bias correction methods, recent studies have put
67 more effort into correcting or reconstructing the inter-variable correlations of climate
68 model outputs. For example, Li et al. (2014) proposed a joint bias correction (JBC)
69 method to correct P and T simultaneously based on a Gaussian copula function, and
70 found that the proposed method is able to reduce the bias of GCM-simulated P-T
71 correlations. Vrac and Friederichs (2015) proposed an empirical copula-bias
72 correction (ECBC) method to adjust the sequence of each GCM-simulated climate
73 variable to match to the corresponding observed sequence, so that the corrected
74 inter-variable, spatial as well as temporal correlations are close to observations.
75 Cannon (2016, 2017) proposed a series of three multivariate bias correction (MBC)
76 methods including MBCp, MBCr, and MBCn to model the inter-variable correlations
77 for climate model outputs. Within these three methods, MBCp and MBCr are two
78 similar methods, both of which combining univariate bias correction and a
79 multivariate linear bias correction algorithm (Bürger et al., 2011) to correct Pearson
80 and Spearman correlation coefficients, respectively. The MBCn method is adapted
81 from an image processing algorithm, and it has been illustrated to effectively reduce
82 the inter-variable correlation bias simulated by climate models, and also has been

83 tested in many impact studies. More recently, Guo et al. (2019) proposed a two-stage
84 quantile mapping (TSQM) method to introduce the observed correlation matrix to
85 climate model outputs by using the distribution-free shuffle algorithm of Iman and
86 Conover (1982). This method can efficiently reconstruct the inter-variable correlation
87 of climate model outputs to match the observations. A comparison with other
88 commonly used methods also showed that the TSQM method consistently performs
89 better with respect to reproducing the observed inter-variable correlations.

90 However, one of the ultimate goals of using multivariate bias correction methods
91 is for hydrological modeling and impact studies. With the development of these new
92 multivariate bias correction techniques, some researchers started to investigate the
93 advantages of using multivariate bias correction methods in hydrological impact
94 studies over the last two years. For example, Chen et al. (2018) compared the
95 hydrological simulation of the independent bias correction (IBC) method and JBC
96 method over 12 watersheds, and found that JBC apparently outperforms IBC for 11
97 out of the 12 watersheds for the calibration period. As for the validation period, the
98 advantages of using JBC are mainly reflected in arid/tropical and
99 snowfall-rainfall-mixed watersheds. Rätty et al. (2018) compared the hydrological
100 simulation of univariate quantile mapping corrected data with two multivariate
101 methods (JBC and MBCn) corrected data over 4 watersheds, and found that the
102 additional benefit of using multivariate bias correction methods is not obvious, and
103 only a slight improvement in simulating snow water equivalents is observed. Seo et al.

104 (2019) investigated the impacts of biased P-T correlation on hydrological variables
105 over two watersheds, and found that the impacts of P-T correlation are more evident
106 on low flow and sub-surface hydrological variables while less remarkable to flow
107 variables with high variability. More recently, Meyer et al. (2019) compared
108 univariate quantile mapping and MBCn in simulating hydrological variables over two
109 alpine catchments. They found that the snow water equivalents, glacier volumes, and
110 streamflow regime simulated using MBCn-corrected data are consistently better than
111 those simulated using univariate quantile mapping corrected data.

112 To date, the investigation of using multivariate bias correction methods in
113 hydrological modeling is just at its infant stage. The above existing studies are
114 fragmented with limitations in the number of catchments and multivariate bias
115 correction methods. The benefits of using multivariate bias correction methods in
116 hydrological impact studies have not been documented, especially in terms of spatial
117 variability. Due to climate diversity in the world, streamflow may show different
118 sensitivities to variations of P, T and their correlations (Berghuijs et al., 2014;
119 Jefferson et al., 2008; Vano et al., 2012). Considering the inadequate representations
120 of the studied watersheds and the uncertainty related to the choice of bias correction
121 methods, it is inappropriate to draw a general conclusion or make a recommendation
122 for using multivariate bias correction methods for hydrological impact studies.

123 Accordingly, this study quantifies the impact of using multivariate bias
124 correction methods on hydrological modeling for North America. The spatial

125 variability is specifically investigated by using 2840 watersheds distributed in
126 different climate regimes over North America. Six state-of-the-art multivariate bias
127 correction methods, including JBC, MBC series, TSQM and ECBC were applied to
128 correct 20 GCM simulations for the selected watersheds. To our knowledge, the
129 selected methods include all newly developed multivariate bias correction methods in
130 the literature. For comparison purposes, a univariate quantile mapping method named
131 as daily bias correction (DBC) (Chen et al., 2013b) was also used.

132 The paper is structured as follows. In the next section, the study area and data are
133 presented. Seven bias correction methods, the hydrological model and the data
134 analysis method are introduced in section 3. The results are shown in section 4, and
135 the discussion and conclusions are presented in section 5 and section 6, respectively.

136 **2. STUDY AREA AND DATA**

137 **2.1 Study area**

138 This study was conducted over 2840 watersheds located in Canada (448
139 watersheds) and the United States (2392 watersheds). These watersheds differ in
140 drainage sizes and climate conditions. The surface area of these watersheds ranges
141 from 302 to 153, 260 km², while the average daily discharge varies from 0.3 to 1886.7
142 m³/s. In terms of climate conditions, the average annual precipitation ranges from 317
143 to 4396 mm, while the average daily temperature ranges from -6.2 to 22.7 °C.
144 According to the Koeppen-Geiger climate classification (Kottek et al., 2006), the

145 2840 watersheds can be divided into 11 climate regimes, covering arid, warm
146 temperate, snow and polar climates. The detailed climate classification and the basic
147 characteristics of each climate regime are shown in Fig. 1 and Table 1, respectively.

148 **2.2 Data**

149 This study used both observed (served as reference data) and climate model
150 simulated daily P, maximum temperature (T_{\max}) and minimum temperature (T_{\min}).
151 Since gridded meteorological data are used in this study, the watershed averaged data
152 for running the hydrological model is calculated by averaging all grid points within
153 and around a watershed. The observed P, T_{\max} , T_{\min} and daily discharge of 448
154 watersheds in Canada were taken from the Canadian Model Parameter Experiment
155 (CANOPEX) database (Arsenault et al., 2016). For the United States, the
156 meteorological data of 2392 watersheds were taken from the Santa Clara daily
157 database (Livneh et al., 2013), while the daily discharge data were extracted from the
158 United States Geological Survey (USGS) database. Considering the uncertainty
159 related to climate models, outputs of 20 GCMs from the Coupled Model
160 Intercomparison Project Phase 5 (CMIP5) (Taylor et al., 2012) were selected. The
161 basic information of these GCMs is presented in Table S1. The daily meteorological
162 data used in this study cover the 1950-2005 period with the first 28 years (1950-1977)
163 used for calibration and the remaining 28 years (1978-2005) used for validation.

164 **3. METHODS**

165 **3.1 Bias correction methods**

166 This study uses 7 bias correction methods, which consist of six multivariate
167 methods (JBC, MBCp, MBCr, MBCn, TSQM, and ECBC), and one univariate
168 method DBC. All these 7 methods are conducted at the daily scale for each specific
169 month. The multivariate bias correction and univariate quantile mapping methods are
170 first calibrated at the calibration period and then applied to the validation period for
171 daily P, T_{\max} and T_{\min} simulated by 20 GCMs over all 2840 watersheds. A summary of
172 these 7 bias correction methods is shown in Table 2, and a more detailed introduction
173 for these 7 methods is provided in the supporting information (Text S1, 3.1.1-3.1.5).

174 **3.2 Hydrological model**

175 The GR4J-9 hydrological model is used for streamflow simulations over 2840
176 watersheds. The GR4J-9 model is a 9-parameter, lumped, conceptual hydrological
177 model, which couples GR4J (Perrin et al., 2003) (5-parameter version) rainfall-runoff
178 model with the CemaNeige (Valéry et al., 2014) (4 parameters) snow accumulation
179 and melt routines.

180 The GR4J model is a soil moisture accounting model, which routes streamflow
181 through two reservoirs and two unit hydrographs. The original version GR4J has four
182 free parameters to be calibrated, which consist of the maximum capacity of the

183 production store, groundwater exchange coefficient, 1-day-ahead maximum capacity
184 of the routing store, and the time base of the unit hydrograph. This model has been
185 tested in a large sample of catchments and shows competitive performances over
186 more complicated models with more parameters (Edijatno et al., 1999;
187 Kunnath-Poovakka & Eldho, 2019). In addition, a previous study (Yang et al., 2019)
188 also showed that the performance of GR4J is more stable than other models (i.e.
189 WASMOD, HBV and XAJ) in a changing climate. In this study, the fixed coefficient
190 in percolation leakage is also set as a free parameter to fit the study area better and is
191 calibrated for each watershed. The potential evaporation in this hydrological model is
192 calculated with the Oudin method (Oudin et al., 2005).

193 Since there is no snow accumulation and snowmelt module in the GR4J model, it
194 cannot be used to watersheds with significant snowmelt over North America.
195 Therefore, a general snow accounting routine named CemaNeige is added. In the
196 CemaNeige module, precipitation is first divided into rainfall and snowfall according
197 to the magnitude of the daily mean temperature, and the potential snowmelt is then
198 computed by a degree-day approach. The CemaNeige module originally has two
199 parameters, one of which is the snowmelt factor and the other is the cold-content
200 factor. To apply this method to calculate the actual daily snowmelt in North America,
201 one parameter for snowpack threshold and the other for the coefficient of actual
202 snowmelt are also required to be calibrated for each watershed.

203 The observed daily P , T_{\max} , T_{\min} and discharge were used to calibrate and validate

204 the GR4J-9 model for all 2840 watersheds. The time periods for calibration and
205 validation are longer than 10 years for all watersheds to obtain reliable parameters. To
206 reduce the influence of non-stationarity of climate time series on model performances,
207 the odd years were used for calibration of the GR4J-9 model and the even years were
208 used for validation (Arsenault et al., 2017). The model parameters were calibrated by
209 the shuffled complex evolution method SCE-UA (Duan et al., 1994), using the
210 Nash-Sutcliffe efficiency (NSE) (Nash & Sutcliffe, 1970) as an objective function.
211 The NSE (shown in Fig. 2) are above 0.5 for all the 2840 watersheds and mainly fall
212 within the range of 0.75-0.85 for calibration and 0.7-0.8 for validation, which
213 indicates the good performance of the GR4J-9 model in the study area.

214 **3.3 Data analysis method**

215 The seven bias correction methods were first evaluated in terms of correcting
216 climate simulations. Since these methods have been extensively evaluated in terms of
217 reproducing the observed marginal distributions (Maraun et al., 2019; Volosciuk et al.,
218 2017), their performances were only demonstrated in terms of correcting the monthly
219 mean value for each variable. In addition, the corrected P-T_{max} and P-T_{min} correlations
220 of monthly time series were presented to demonstrate the performance of each method
221 in correcting the inter-variable correlations. The Spearman correlation coefficient was
222 used as it has no requirement for a particular distribution. The root-mean-square-error
223 (RMSE) was calculated for each climate criterion against the climate reference data

224 over all watersheds.

225 In terms of evaluating the hydrological simulations, the first two years of the
226 simulations are regarded as a warming up period and removed from both calibration
227 (removing 1950-1951) and validation (removing 1978-1979) periods before the
228 evaluation. Three hydrological state variables including the winter snow proportion,
229 the spring daily mean snowmelt and the summer wet-day potential evaporation were
230 used as the evaluation metrics. In addition, these methods are also evaluated with
231 respect to driving the hydrological model to simulate monthly mean flow, high flow
232 and low flow, and time variables (e.g. time to the peak discharge, and time to the
233 beginning and the end of the annual maximum flood). Time to the beginning and to
234 the end of the flood is calculated based on the cumulative annual hydrograph of each
235 watershed. Specifically, four breakpoints in the cumulative annual hydrograph are
236 picked out and connected by straight lines, aiming at minimizing the RMSE error with
237 the original cumulative annual hydrograph. The number of days from the beginning of
238 the year to reach the first breakpoint is then defined as the beginning of the flood, and
239 the number of days to reach the second breakpoint is defined as the end of the flood.
240 The procedures for calculating the time of the beginning and end of the flood is
241 presented in Fig. S1 in the supporting information. The same method was also used in
242 Chen et al. (2011, 2018). To quantify the results, absolute error (AE), absolute relative
243 error (ARE) and RMSE were also calculated for the simulated hydrological variables
244 against the hydrological variables simulated using climate reference data. The

245 summary and definitions of climatic and hydrological metrics are shown in Table S2.

246 To statistically test the impacts of using multivariate bias correction methods
247 relative to the univariate quantile mapping method in hydrological modeling, the
248 analysis of variance (ANOVA) and Dunnett-t test (Dunnett, 1955) were conducted
249 based on RMSE of multivariate bias-corrected simulations and univariate
250 bias-corrected simulations for each hydrological variable. The Dunnett-t test is a
251 multiple comparison method designed for comparing the difference in the mean value
252 of the control group and multiple experimental groups. In the Dunnett-t test, the
253 RMSE derived from DBC (20 values for 20 GCMs) is regarded as the control group,
254 and the RMSE derived from each of 6 multivariate methods were compared with the
255 control group. If the P-value of the Dunnett-t test was smaller than 0.1, the results of
256 the multivariate method are considered to be significantly different from the DBC
257 method. To show the reliability of the Dunnett-t test, the statistical power was also
258 calculated for those tests whose P-value was smaller than 0.1.

259 **4. RESULTS**

260 **4.1 Observed P-T dependence**

261 To show the variation of the P-T dependence in terms of climate regimes and
262 seasons, the mean observed $P-T_{\max}$ and $P-T_{\min}$ Spearman correlation coefficients are
263 calculated for the watersheds from 11 climate regimes for each month and for both
264 1950-1977 and 1978-2005 periods (Fig. S2). Results show that the $P-T_{\max}$ and $P-T_{\min}$

265 correlations varied greatly with climate regimes and seasons. For arid climate BSk
266 and warm temperate climate Csa and Csb, the $P-T_{\max}$ correlations are negative for all
267 months, while for most of the rest climate regimes, the $P-T_{\max}$ correlations are mostly
268 negative in summer and positive in winter. For the Dfa climate, the $P-T_{\max}$ correlation
269 in summer is weak and the correlation coefficient is near 0. In terms of $P-T_{\min}$
270 correlation, almost all the climate regimes show a positive result for all months except
271 for the negative $P-T_{\min}$ correlation of the Csa climate in April and May. Apart from the
272 variation of P-T correlation in climate regimes and seasons, nonstationarity of the
273 observed correlation coefficient was also observed between these two continuous time
274 periods. For example, the negative $P-T_{\max}$ correlations for Csa climate in March and
275 April are apparently weakened from 1950-1977 to 1978-2005 periods. All these
276 results emphasize the necessity to analyze the spatial variability of using multivariate
277 bias correction methods for hydrological modeling.

278 **4.2 Climate simulations**

279 4.2.1 The performance in representing the univariate distributional characteristics

280 The RMSE of the monthly mean values of corrected P, T_{\max} and T_{\min} are
281 presented as boxplot in Fig. 3 for 4 typical months over 2840 watersheds for the
282 validation period. Each box is constructed by 20 RMSE values of 20 GCMs. Results
283 show that the univariate quantile mapping method and the six multivariate bias
284 correction methods perform similarly in correcting the monthly mean of precipitation

285 and temperature for all 4 months. In addition, all these 7 methods show smaller
286 RMSE value and smaller uncertainty related to GCMs in July but show larger RMSE
287 value and larger uncertainty in January for all three variables.

288 4.2.2 Performance in correcting the inter-variable correlation

289 Fig. 4 present the spatial distribution of corrected $P-T_{\max}$ correlation coefficients
290 for July at the validation period. The climate model BCC-CSM1.1 (m) is used as an
291 example to demonstrate the results. Observed $P-T_{\max}$ correlation coefficients are also
292 plotted for comparison. Results show that the DBC method cannot reproduce the
293 observed $P-T_{\max}$ correlation coefficients, whose results are similar to correlation
294 coefficients of the raw climate model (results not shown). For the 6 multivariate
295 methods, MBC series, TSQM and ECBC methods have similar performances and all
296 properly reproduce the observed $P-T_{\max}$ correlation coefficients, though the MBCp
297 method is slightly worse. However, the JBC method has limited capability to correct
298 the simulated $P-T_{\max}$ correlation coefficients, and it has no apparent advantage over
299 the DBC method. The results are also presented in Fig. S3 for January at the
300 validation period. Generally, the performance of each method in January is similar to
301 that in July.

302 The RMSEs of the inter-variable correlations of corrected time series over 2840
303 watersheds are shown in Fig. 5 for 20 GCMs. Results are shown as boxplots for 4
304 typical months and both calibration and validation periods. Similarly, each box
305 consists of 20 values corresponding to 20 GCMs. Results show that DBC has the

306 largest RMSE among all methods. For the 6 multivariate methods, the JBC method
307 shows the largest RMSE, which has also been shown in the spatial distribution of the
308 corrected P-T_{max} correlation coefficients in Figs. 4 and S3. For the other 5 multivariate
309 methods, MBCn, TSQM, and ECBC perform similarly and better than the other two
310 methods in terms of the RMSE for both calibration and validation periods.

311 **4.3 Hydrological simulations**

312 4.3.1 Performance in simulating hydrological state variables

313 Fig. 6 presents the mean AE of winter snow proportion calculated using climate
314 model simulations with and without bias correction across 20 GCMs over all
315 watersheds for the validation period. Results show that AEs of the proportional
316 precipitation in snow as simulated by the raw GCMs are greatest in the temperate
317 climate zone (mostly between 32 and 48N), and lowest to both north and south of the
318 zone due to all snowfall in the former and all rainfall in the latter in winter, indicating
319 that the bias correction of P-T correlation is essential for properly simulating winter
320 hydrology in the temperate zones. The use of univariate DBC method can improve the
321 winter snow proportion simulation, especially for the central United States. The
322 multivariate methods can further reduce the AE of the winter snow proportion
323 simulation. For example, the AE in the northeastern United States reduces from
324 around 8-10% when using DBC to 1-3 % when using TSQM. The reduction of AE
325 indicates that the use of multivariate methods is able to better distinguish the snowfall

326 from the rainfall in winter.

327 Fig. 7 presents the mean ARE of spring daily mean snowmelt calculated using
328 climate model simulations with and without bias correction across 20 GCMs over all
329 watersheds for the validation period. Results show that the spring daily mean
330 snowmelt simulated by DBC-corrected data are more accurate compared to the raw
331 GCMs data, especially for most northern watersheds. The multivariate methods
332 consistently perform better than the DBC method with respect to reproducing the
333 spring daily snowmelt calculated using observed data, especially for central North
334 America. For example, the ARE in the central continent reduced from 32-40 % when
335 using DBC to 4-16 % when using MBCn.

336 Fig. 8 presents the difference between dry-day and wet-day potential evaporation
337 (dry days minus wet days) in summer, calculated using reference data and 20
338 corrected GCMs simulations over all watersheds for the validation period. For
339 reference data, the evaporation in dry days is lower than that in wet days in eastern
340 North America as indicated by the red color in this area, while an opposite pattern is
341 observed in western North America. This phenomenon is consistent with the observed
342 P-T correlations of these two regions in summer. Fig. S4 shows the observed
343 correlation between P and daily mean temperature (T_{mean}) of the validation period
344 over the 2840 watersheds for each month. For the eastern region, P and T_{mean} are
345 positively correlated in summer, which results in that the evaporation in dry days is
346 lower than in wet days. However, for the western region, the correlation between P

347 and T_{mean} in summer is mostly negative, which results in that the evaporation in dry
348 days are higher than in wet days. Generally, all bias correction methods can represent
349 this pattern. However, the DBC method fails to capture the positive difference in
350 Canada and the negative difference in the southeastern United States. The JBC and
351 MBCp methods also cannot capture the differences in these two regions. However, the
352 rest of multivariate methods (MBCr, MBCn, TSQM and ECBC) more properly
353 reproduce the observed pattern of the difference between dry and wet day potential
354 evaporation.

355 Fig. 9 presents the Dunnett-t test of RMSE between the DBC and multivariate
356 methods for simulating three hydrological state variables. The blue color represents
357 the fact that the multivariate methods perform significantly better than the DBC at the
358 significance level of 10%, while the red color represents the opposite result, and the
359 white color represents there is no significant difference between these two methods.
360 For the winter snowfall proportion (Fig. 9(a) and (b)), the multivariate methods
361 perform significantly better than the DBC method for almost all climate regimes and
362 for both calibration and validation periods. There are only two cases (the Dfa in the
363 calibration period and the Csa in the validation period) that the TSQM method
364 performs significantly worse than the DBC method. For the spring daily mean
365 snowmelt (Fig. 9(c) and (d)), the multivariate methods consistently outperform the
366 DBC method over almost all climate regimes for the calibration period, but for the
367 validation period, the results are dependent on climate regimes. Specifically, the

368 multivariate methods perform significantly better for arid climate (BSk) and warm
369 temperate climate (Cfa, Cfb, and Csb). However, for most snow climate (Dfb, Dfc,
370 Dsb and Dsc) and polar climate (ET), the multivariate methods perform similarly to or
371 even worse than the DBC method. For the mean wet-day evaporation in summer (Fig.
372 9(e) and (f)), five out of six multivariate methods show significantly better
373 performance than the DBC method for all climate regimes in calibration period, and
374 the advantages of multivariate methods are weakened when comes to the validation
375 period. However, an exception is observed when using the JBC method, which
376 demonstrates the incapability of this method in correcting the P-T correlation in
377 summer as indicated in Fig. 4.

378 4.3.2 Performance in simulating streamflow variables

379 Fig. 10 presents the Dunnett-t test for RMSE of the mean streamflow over 11
380 climate regimes for 4 seasons of the calibration and validation periods. Prior to using
381 the Dunnett-t test, the 12 monthly RMSEs of the mean streamflow were averaged to
382 obtain 4 seasonal values. For the calibration period, the multivariate methods
383 consistently perform better than or comparable to the DBC method in simulating the
384 mean streamflow over all climate regimes and 4 seasons, though a few of
385 disadvantages were also observed. For the validation period, the advantages of using
386 multivariate methods are generally not significant, even though the performances of
387 these methods are climate-and season-dependent. For the arid climate and warm
388 temperate climate, the multivariate methods do not show significant differences with

389 the DBC method for almost all 4 seasons, and only two cases that multivariate
390 methods perform better than the univariate counterpart in winter. However, for
391 snow-characterized climate, the performance of multivariate methods differs between
392 spring-summer and autumn-winter. Multivariate methods show advantages in
393 simulating the mean streamflow in autumn and winter for snow climate, while
394 showing comparable or even worse performances in spring and summer. For polar
395 climate, the performances of multivariate and univariate bias correction methods are
396 generally comparable for all 4 seasons.

397 Fig. 11 presents the Dunnett-t test results for RMSE of high flow and low flow
398 over all 11 climate regimes for both calibration and validation periods. In simulating
399 the high flow, multivariate methods perform better than the DBC method for most
400 climate regimes, while several worse cases are exhibited for JBC and TSQM methods.
401 However, in the validation period, the multivariate methods do not show advantages
402 over the univariate DBC method, and on the contrary, these methods even perform
403 worse than the univariate DBC method for specific climate regimes (e.g. ECBC in the
404 Csb climate and JBC in the Dfc climate). In simulating the low flow, multivariate
405 methods significantly perform better than DBC over most climate regimes (except for
406 arid climate BSk) for the calibration period, with the exception of the TSQM method.
407 In the validation period, the advantages of using multivariate methods are not
408 apparent, and the multivariate methods show comparable performances with the DBC
409 method with both advantages and disadvantages were observed.

410 The Dunnett-t test for RMSE of time variables is shown in Fig. 12 over all 11
411 climate regimes for both calibration and validation periods. Similar to other
412 hydrological variables, the multivariate methods significantly outperform the DBC
413 over most climate regimes for the calibration period, especially for simulating the
414 time to the peak discharge. In simulating the time to the beginning and end of the
415 flood, the advantages of multivariate methods were mostly observed in
416 snow-characterized and polar climates. For the validation period, the advantages of
417 using multivariate methods are not very significant. Significant advantages are
418 observed for simulating the time to the peak discharge and time to the beginning of
419 flood for warm temperate Csb, and simulating time to the end of flood for polar
420 climate ET.

421 To show the reliability of the hypothesis testing results, the statistical power is
422 calculated for the Dunnett-t test that shows significant differences between
423 multivariate and univariate methods for hydrological variables. The statistical power
424 values are shown as boxplots in Fig. S5. For the calibration period, the mean values of
425 statistical power are greater than 0.9 for all six types of hydrological variables, and the
426 values for three state variables are greater than those of streamflow variables. For the
427 validation period, the mean values of statistical power are greater than 0.8 except for
428 the mean flow whose mean value ranges between 0.6 and 0.7. These high values of
429 statistical power prove the rationality of the hypothesis testing used in this study.

430 The hypothesis testing shows that multivariate bias correction methods can

431 significantly improve the simulation of the streamflow for the calibration period, but
432 do not show many significant advantages for the validation period. To investigate the
433 effects of using multivariate methods more explicitly in simulating the streamflow for
434 the validation period, the mean values of the RMSE (20 values of 20 GCMs) of each
435 multivariate method are also compared to the corresponding mean RMSE values of
436 DBC for each streamflow variable (Fig. S6). The ratio (%) that the mean values of
437 RMSE derived from the multivariate methods being smaller than those derived from
438 DBC in simulating each hydrological variable for each climate regime is also
439 calculated and shown in Table 3. The results show that the multivariate methods have
440 smaller RMSE than DBC in simulating most streamflow variables for the validation
441 period with the ratio ranging from 55-82%, except for summer mean flow with the
442 ratio of 27%. In terms of climate regimes, the ratio that multivariate methods showing
443 advantages is higher for arid and warm temperature climates whose value is 70% and
444 71%, respectively. However, for snow and polar climates, the performances of
445 multivariate methods are generally comparable to those of DBC with the advantage
446 ratios of 54% and 55%, respectively. Overall, these comparisons illustrate that the
447 multivariate methods generally perform better than the univariate counterparts at
448 simulating the streamflow variables for the validation period, even though these
449 advantages do not reach a significant level when using the hypothesis testing. In
450 addition, the multivariate methods perform better than the univariate counterpart in
451 streamflow simulations for arid and warm temperate climate regimes located in

452 southern regions.

453 **5. DISCUSSION**

454 This study quantifies the impacts of using multivariate bias correction methods
455 on hydrological modeling and investigates their spatial variability by using 2840
456 watersheds distributed in different climate regimes over North America. Results show
457 that the multivariate bias correction methods significantly outperform the univariate
458 bias correction method in simulating hydrological variables for the calibration period.
459 As for the validation period, the advantages of multivariate methods are not as
460 profound as for the calibration period. But they are still significant for the
461 hydrological state variables, while statistically insignificant for streamflow variables
462 for most climate regimes based on the Dunnett-t test. However, the direct
463 comparisons using RMSE show the multivariate methods still perform better than the
464 univariate method in streamflow simulations in general.

465 Compared to the commonly used univariate quantile mapping method, the
466 multivariate bias correction methods are able to adjust the biased inter-variable
467 correlations simulated by climate models. Therefore, the necessity of using
468 multivariate bias correction methods for hydrological modeling depends on the biases
469 of inter-variable correlations simulated by climate models for a specific region. The
470 performance of GCM in simulating the inter-variable correlations of climate variables
471 is regionally dependent. Fig. S7 presents the mean absolute relative error (MARE) of

472 monthly $P-T_{\max}$ and $P-T_{\min}$ correlation coefficient simulated by 20 GCMs over 11
473 climate regimes for both calibration and validation periods. Results show that
474 GCM-simulated $P-T_{\max}$ correlations are mostly biased for warm temperate climate
475 regime in summer while for snow and polar climate regime in winter. For the $P-T_{\min}$
476 correlations, biases are mostly observed for arid climate and polar climate regimes. It
477 is easy to find that multivariate methods show apparent advantages in simulating the
478 mean streamflow for regions (as shown in Fig. 10) where climate models are more
479 biased in simulating inter-variables correlations (as shown in Fig. S7). Specifically,
480 the multivariate methods show apparent advantages for the warm temperate climate in
481 summer as well as for snow climate in winter in the calibration period. This example
482 further proves that the correction of biased $P-T$ correlation is able to improve the
483 simulation of mean streamflow. Due to the complex terrain or inadequate
484 representation of basic physical processes for some regions, the climate model may
485 show a low capability to simulate the inter-variable correlations and thus results in
486 large biases. For these regions, it is clearly necessary to use multivariate methods for
487 hydrological impact studies.

488 This study shows that the multivariate bias correction methods significantly
489 outperform the univariate method in simulating most hydrological variables for the
490 calibration period, but these advantages are weakened for most climate regimes and
491 hydrological variables when coming to the validation period, especially for
492 streamflow variables. This may be because the bias of inter-variable correlation

493 simulated by climate models is not stationary, and the observed inter-variable
494 correlation itself is also not invariable. Previous studies (Chen et al., 2017; Hui et al.,
495 2018; Maraun, 2012) have shown that bias correction methods can deteriorate the
496 original climate simulations when bias directions are different between future and
497 historical periods (or calibration and validation periods) or when future biases reduce
498 to less than half the calibration biases. The nonstationarity of inter-variable correlation
499 bias of climate models can be observed in Fig. S7. For example, larger P-T_{max}
500 correlation bias is observed for the Dfa climate in summer for the 1978-2005 period
501 compared to the 1950-1977 period. Besides the nonstationarity of model bias, the
502 variation of observed inter-variable correlations also results in the weakened
503 performance of multivariate methods. To further explore this problem, Fig. S8
504 presents the differences of observed monthly P-T_{max} correlation coefficient between
505 1950-1977 and 1978-2005 period for all 2840 watersheds in North America. Results
506 show that the observed P-T_{max} correlation changes considerably for most watersheds
507 and months. For some watersheds, these changes can be larger than 0.3 in either
508 positive or negative. However, all existing multivariate bias correction methods only
509 introduce the correlation coefficients at the calibration period to the validation period
510 or future period. In other words, the nonstationarity of inter-variable correlations is
511 not considered. This partly explains why the advantages of using multivariate bias
512 correction methods in the calibration period may even reverse when comes to the
513 validation period. Berg et al. (2015) found that due to global warming, large parts of

514 the land surface show more significantly negative summer P-T correlations for the
515 2071-2100 period than for the 1971-2000 period. However, in some other areas, the
516 P-T correlations in summer may also become significantly more positive. Mahony
517 and Cannon (2018) also found that the P-T correlation may change more obviously in
518 the future due to natural variability and climate sensitivity. More recently, Hao et al.
519 (2019) found that the P-T correlation would be influenced by global warming and
520 thus may result in new compound extreme events in the future. However, most GCMs
521 show a limited capability to simulate the changes in P-T correlations. With the
522 continuous change of temperature in the foreseeable future, the P-T correlation may
523 vary with time, which may challenge the multivariate bias correction methods that
524 reproducing the historical correlation for the future. To deal with this problem,
525 multivariate bias correction methods taking into account the nonstationarities of
526 model biases as well as inter-variable correlations need to be developed. This may be
527 an avenue for future studies. In addition, the different performances of the
528 hydrological model between the calibration and validation periods (Fig. 2) may also
529 contribute to the weakened performances of the multivariate methods in the validation
530 period.

531 Apart from the stationary assumption of the inter-variable correlations, most
532 multivariate bias correction methods involve modifying the time sequence of the
533 simulated variable to induce the desired correlation matrix. Fig. S9 in the supporting
534 information presents the Spearman correlation coefficients between the corrected and

535 raw climate model-simulated variables for July over both calibration and validation
536 periods, using BCC-CSM1.1(m) as an example. Results show that, DBC-and
537 JBC-corrected data have the highest correlation coefficient with the raw data, as these
538 two methods do not alter the time sequence of the raw climate model data. Only the
539 correlation of precipitation between the corrected and raw data is slightly reduced due
540 to the correction of the wet-day frequency and the different correction factors in each
541 quantile. The three MBC methods adjust the time sequence of the raw model data
542 when inducing the desired correlation matrix. The impacts on correlations are
543 dependent on the adjustment of the temporal sequence. MBC-corrected simulations
544 have high correlation coefficients with the raw data for all three variables. The TSQM
545 method keeps the original simulated time sequence of precipitation while re-ranks the
546 temperature sequence, so it has high correlation coefficients for precipitation but low
547 correlation coefficients for temperature with raw model data. The ECBC method
548 reorders the original time sequence of each simulated variable to match the sequence
549 of historical observations, which loses the sequence information of the model outputs,
550 thus the correlation coefficients between ECBC-corrected and raw model data are
551 nearly 0. By definition, all MBC, TSQM and ECBC modify the temporal sequence of
552 the climate model outputs to induce the desired inter-variable correlations. However,
553 ECBC assumes the temporal sequence of climate simulations is identical to historical
554 observations. This assumption may not be valid in a changing climate, as the temporal
555 sequence likely changes for the future period. In contrast, the MBC method does not

556 rely on this assumption and allows the rank orders of climate data to evolve over time,
557 and the TSQM method has a similar feature to allow the rank order of a key climate
558 variable to evolve with time. For the JBC method, though it does not involve
559 modifying the time sequence and maintains the original rank orders equally to the
560 univariate DBC method, it does not show significant advantages over the DBC
561 method for the validation period. The similar performances of DBC and JBC partially
562 reflect the fact that the additional parameters and processes in JBC may not help much
563 in improving the hydrological simulations for the validation period.

564 There is also a limitation in this study that needs to be acknowledged. Due to the
565 computational load for a large domain over North America, only one lumped
566 hydrological model was used. The use of a more physical-based land surface or
567 hydrological model can further take advantages of the spatial dependence of
568 cross-correlated multiple climate variables. This can be an avenue for future studies.

569 **6. CONCLUSIONS**

570 In this study, the impacts of using state-of-the-art multivariate bias correction
571 methods on hydrological modeling were investigated over 2840 watersheds in North
572 America. The main conclusions are summarized as follows:

573 (1) Most multivariate bias correction methods can effectively reproduce the
574 observed inter-variable correlation coefficient for the watersheds in North America,
575 while the univariate bias correction method shows limited ability in this aspect.

576 (2) In terms of hydrological modeling, the use of multivariate bias correction
577 methods can significantly improve the simulation of hydrological variables for most
578 climate regimes in the calibration period. However, the advantages of using
579 multivariate methods in the validation period are not as profound as for the calibration
580 period, especially for simulating streamflow variables, because of the non-stationarity
581 of the inter-variable correlations.

582 (3) The advantage of using multivariate bias correction methods for hydrological
583 modeling is region-dependent. In general, the multivariate methods show more
584 advantages in arid and warm temperate climate regimes mainly in the southern
585 regions, while showing fewer advantages in snow-characterized and polar climate
586 regimes mainly in the northern regions. This regional difference is more obvious for
587 the validation period.

588 (4) In terms of the performances of 6 multivariate bias correction methods, the
589 MBC series and ECBC method show more advantages over univariate DBC method
590 in simulating hydrological variables in North America, while JBC and TSQM show
591 limited advantages, especially in simulating streamflow variables.

592 **Acknowledgments:**

593 This work was partially supported by the National Natural Science Foundation of
594 China (Grant no. 51779176, 51539009), the National Key Research and Development
595 Program of China (No. 2017YFA0603704), the Overseas Expertise Introduction

596 Project for Discipline Innovation (111 Project) funded by Ministry of Education and
597 State Administration of Foreign Experts Affairs P.R. China (Grant No. B18037), and
598 the Thousand Youth Talents Plan from the Organization Department of CCP Central
599 Committee (Wuhan University, China).

600 The authors would like to thank Dr. Chao Li at the University of Victoria for
601 providing scripts of the JBC method and Dr. Alex Cannon at the Environment and
602 Climate Change Canada (Climate Research Division) for publishing scripts of MBCp,
603 MBCr and MBCn methods. The authors would also like to thank Dr. Arsenault at the
604 University of Quebec, and Dr. Livneh at the University of Colorado Boulder and Dr.
605 Maurer at Santa Clara University for making their data (CANOPEX and Santa Clara
606 database, respectively) available, and these data can be accessed as guided in their
607 articles. The authors would like to acknowledge the contribution of the USGS, and the
608 World Climate Research Program Working Group on Coupled Modelling, and to
609 thank the climate modeling groups listed in Table S1 for producing and making their
610 model outputs available. The URIs of these data are as follows:

611 CANOPEX: (<http://canopex.etsmtl.net>)

612 Santa Clara database:

613 (<ftp://livnehpublicstorage.colorado.edu/public/Livneh.2013.CONUS.Dataset/>)

614 USGS database: (<https://www.usgs.gov/>)

615 CMIP5 database: (<https://www.wcrp-climate.org/wgcm-cmip/wgcm-cmip5>)

616 **References**

- 617 Arsenault, R., Bazile, R., Ouellet Dallaire, C., & Brissette, F. (2016). CANOPEX: A
618 Canadian hydrometeorological watershed database. *Hydrological Processes*,
619 30(15), 2734-2736. doi:10.1002/hyp.10880
- 620 Arsenault, R., Essou, G. R. C., & Brissette, F. P. (2017). Improving Hydrological Model
621 Simulations with Combined Multi-Input and Multimodel Averaging
622 Frameworks. *Journal of Hydrologic Engineering*, 22(4), 04016066.
623 doi:10.1061/(asce)he.1943-5584.0001489
- 624 Bürger, G., Schulla, J., & Werner, A. T. (2011). Estimates of future flow, including
625 extremes, of the Columbia River headwaters. *Water Resources Research*,
626 47(10). doi:10.1029/2010wr009716
- 627 Berg, A., Lintner, B. R., Findell, K., Seneviratne, S. I., van den Hurk, B., Ducharne, A.,
628 Chéruiy, F., Hagemann, S., Lawrence, D. M., Malyshev, S., Meier, A., &
629 Gentine, P. (2015). Interannual Coupling between Summertime Surface
630 Temperature and Precipitation over Land: Processes and Implications for
631 Climate Change*. *Journal of Climate*, 28(3), 1308-1328.
632 doi:10.1175/jcli-d-14-00324.1
- 633 Berghuijs, W. R., Woods, R. A., & Hrachowitz, M. (2014). A precipitation shift from
634 snow towards rain leads to a decrease in streamflow. *Nature Climate Change*,
635 4(7), 583-586. doi:10.1038/nclimate2246
- 636 Cannon, A. J. (2016). Multivariate Bias Correction of Climate Model Output: Matching

637 Marginal Distributions and Intervariable Dependence Structure. *Journal of*
638 *Climate*, 29(19), 7045-7064. doi:10.1175/jcli-d-15-0679.1

639 Cannon, A. J. (2017). Multivariate quantile mapping bias correction: an N-dimensional
640 probability density function transform for climate model simulations of
641 multiple variables. *Climate Dynamics*, 50(1-2), 31-49.
642 doi:10.1007/s00382-017-3580-6

643 Cannon, A. J., Sobie, S. R., & Murdock, T. Q. (2015). Bias Correction of GCM
644 Precipitation by Quantile Mapping: How Well Do Methods Preserve Changes
645 in Quantiles and Extremes? *Journal of Climate*, 28(17), 6938-6959.
646 doi:10.1175/jcli-d-14-00754.1

647 Chen, J., Brissette, F. P., Poulin, A., & Leconte, R. (2011). Overall uncertainty study
648 of the hydrological impacts of climate change for a Canadian watershed. *Water*
649 *Resources Research*, 47, W12509, doi: :10.1029/2011WR010602

650 Chen, J., Brissette, F. P., Chaumont, D., & Braun, M. (2013a). Finding appropriate bias
651 correction methods in downscaling precipitation for hydrologic impact studies
652 over North America. *Water Resources Research*, 49(7), 4187-4205.
653 doi:10.1002/wrcr.20331

654 Chen, J., Brissette, F. P., Chaumont, D., & Braun, M. (2013b). Performance and
655 uncertainty evaluation of empirical downscaling methods in quantifying the
656 climate change impacts on hydrology over two North American river basins.
657 *Journal of Hydrology*, 479, 200-214. doi:10.1016/j.jhydrol.2012.11.062

658 Chen, J., Brissette, F. P., Liu, P., & Xia, J. (2017). Using raw regional climate model
659 outputs for quantifying climate change impacts on hydrology. *Hydrological*
660 *Processes*, 31(24), 4398-4413. doi:10.1002/hyp.11368

661 Chen, J., Li, C., Brissette, F. P., Chen, H., Wang, M., & Essou, G. R. C. (2018). Impacts
662 of correcting the inter-variable correlation of climate model outputs on
663 hydrological modeling. *Journal of Hydrology*, 560, 326-341.
664 doi:10.1016/j.jhydrol.2018.03.040

665 Duan, Q., Sorooshian, S., & Gupta, V. K. (1994). Optimal use of the SCE-UA global
666 optimization method for calibrating watershed models. *Journal of Hydrology*,
667 158(3-4), 265-284. doi:10.1016/0022-1694(94)90057-4

668 Dunnett C.W. (1955) A multiple comparison procedure for comparing several
669 treatments with a control. *J Am Stat Assoc* 50(272):1096–1121

670 Edijatno, De Oliveira Nascimento, N., Yang, X., Makhoulouf, Z., & Michel, C. (1999).
671 GR3J: a daily watershed model with three free parameters. *Hydrological*
672 *Sciences Journal*, 44(2), 263-277. doi:10.1080/02626669909492221

673 Guo, Q., Chen, J., Zhang, X., Shen, M., Chen, H., & Guo, S. (2019). A new two-stage
674 multivariate quantile mapping method for bias correcting climate model outputs.
675 *Climate Dynamics*, 53(5-6), 3603-3623. doi:10.1007/s00382-019-04729-w

676 Gutiérrez, J. M., Maraun, D., Widmann, M., Huth, R., Hertig, E., Benestad, R., Roessler,
677 O., Wibig, J., Wilcke, R., Kotlarski, S., San Martín, D., Herrera, S., Bedia, J.,
678 Casanueva, A., Manzananas, R., Iturbide, M., Vrac, M., Dubrovsky, M.,

679 Ribalaygua, J., Pórtoles, J., Rätty, O., Räisänen, J., Hingray, B., Raynaud, D.,
680 Casado, M. J., Ramos, P., Zerenner, T., Turco, M., Bosshard, T., Štěpánek, P.,
681 Bartholy, J., Pongracz, R., Keller, D. E., Fischer, A. M., Cardoso, R. M., Soares,
682 P. M. M., Czernecki, B., & Pagé, C. (2019). An intercomparison of a large
683 ensemble of statistical downscaling methods over Europe: Results from the
684 VALUE perfect predictor cross-validation experiment. *International Journal of*
685 *Climatology*, 39(9), 3750-3785. doi:10.1002/joc.5462

686 Hakala, K., Addor, N., & Seibert, J. (2018). Hydrological Modeling to Evaluate
687 Climate Model Simulations and Their Bias Correction. *Journal of*
688 *Hydrometeorology*, 19(8), 1321-1337. doi:10.1175/jhm-d-17-0189.1

689 Hao, Z., Phillips, T. J., Hao, F., & Wu, X. (2019). Changes in the dependence between
690 global precipitation and temperature from observations and model simulations.
691 *International Journal of Climatology*. doi:10.1002/joc.6111

692 Hui, Y., Chen, J., Xu, C. Y., Xiong, L., & Chen, H. (2018). Bias nonstationarity of
693 global climate model outputs: The role of internal climate variability and
694 climate model sensitivity. *International Journal of Climatology*, 39(4),
695 2278-2294. doi:10.1002/joc.5950

696 Iman, R. L., & Conover, W. J. (1982). A distribution-free approach to inducing rank
697 correlation among input variables. *Communications in Statistics - Simulation*
698 *and Computation*, 11(3), 311-334.

699 Jefferson, A., Nolin, A., Lewis, S., & Tague, C. (2008). Hydrogeologic controls on

700 streamflow sensitivity to climate variation. *Hydrological Processes*, 22(22),
701 4371-4385. doi:10.1002/hyp.7041

702 Kottek, M., Grieser, J., Beck, C., Rudolf, B., & Rubel, F. (2006). World Map of the
703 Köppen-Geiger climate classification updated. *Meteorologische Zeitschrift*,
704 15(3), 259-263. doi:10.1127/0941-2948/2006/0130

705 Kumar, D., Kodra, E., & Ganguly, A. R. (2014). Regional and seasonal
706 intercomparison of CMIP3 and CMIP5 climate model ensembles for
707 temperature and precipitation. *Climate Dynamics*, 43(9-10), 2491-2518.
708 doi:10.1007/s00382-014-2070-3

709 Kunnath-Poovakka, A., & Eldho, T. I. (2019). A comparative study of conceptual
710 rainfall-runoff models GR4J, AWBM and Sacramento at catchments in the
711 upper Godavari river basin, India. *Journal of Earth System Science*, 128(2).
712 doi:10.1007/s12040-018-1055-8

713 Li, C., Sinha, E., Horton, D. E., Diffenbaugh, N. S., & Michalak, A. M. (2014). Joint
714 bias correction of temperature and precipitation in climate model simulations.
715 *Journal of Geophysical Research: Atmospheres*, 119(23), 13,153-113,162.
716 doi:10.1002/2014jd022514

717 Li, W., Chen, J., Li, L., Chen, H., Liu, B., Xu, C.-Y., & Li, X. (2019). Evaluation and
718 bias correction of S2S precipitation for hydrological extremes. *Journal of*
719 *Hydrometeorology*. doi:10.1175/jhm-d-19-0042.1

720 Livneh, B., Rosenberg, E. A., Lin, C., Nijssen, B., Mishra, V., Andreadis, K. M.,

721 Maurer, E. P., & Lettenmaier, D. P. (2013). A Long-Term Hydrologically Based
722 Dataset of Land Surface Fluxes and States for the Conterminous United States:
723 Update and Extensions. *Journal of Climate*, 26(23), 9384-9392.
724 doi:10.1175/jcli-d-12-00508.1

725 Mahony, C. R., & Cannon, A. J. (2018). Wetter summers can intensify departures from
726 natural variability in a warming climate. *Nat Commun*, 9(1), 783.
727 doi:10.1038/s41467-018-03132-z

728 Maraun, D. (2012). Nonstationarities of regional climate model biases in European
729 seasonal mean temperature and precipitation sums. *Geophysical Research*
730 *Letters*, 39(6). doi:10.1029/2012gl051210

731 Maraun, D. (2016). Bias Correcting Climate Change Simulations - a Critical Review.
732 *Current Climate Change Reports*, 2(4), 211-220.
733 doi:10.1007/s40641-016-0050-x

734 Maraun, D., Widmann, M., & Gutiérrez, J. M. (2019). Statistical downscaling skill
735 under present climate conditions: A synthesis of the VALUE perfect predictor
736 experiment. *International Journal of Climatology*, 39(9), 3692-3703.
737 doi:10.1002/joc.5877

738 Mehran, A., AghaKouchak, A., & Phillips, T. J. (2014). Evaluation of CMIP5
739 continental precipitation simulations relative to satellite-based gauge-adjusted
740 observations. *Journal of Geophysical Research: Atmospheres*, 119(4),
741 1695-1707. doi:10.1002/2013jd021152

742 Meyer, J., Kohn, I., Stahl, K., Hakala, K., Seibert, J., & Cannon, A. J. (2019). Effects of
743 univariate and multivariate bias correction on hydrological impact projections
744 in alpine catchments. *Hydrology and Earth System Sciences*, 23(3), 1339-1354.
745 doi:10.5194/hess-23-1339-2019

746 Nash, J. E., & Sutcliffe, J. V. (1970). River flow forecasting through conceptual models
747 part I — A discussion of principles. *Journal of Hydrology*, 10(3), 282-290.
748 doi:10.1016/0022-1694(70)90255-6

749 Oudin, L., Hervieu, F., Michel, C., Perrin, C., Andréassian, V., Anctil, F., & Loumagne,
750 C. (2005). Which potential evapotranspiration input for a lumped rainfall–
751 runoff model? *Journal of Hydrology*, 303(1-4), 290-306.
752 doi:10.1016/j.jhydrol.2004.08.026

753 Perrin, C., Michel, C., & Andréassian, V. (2003). Improvement of a parsimonious
754 model for streamflow simulation. *Journal of Hydrology*, 279(1-4), 275-289.
755 doi:10.1016/s0022-1694(03)00225-7

756 Rätty, O., Räisänen, J., Bosshard, T., & Donnelly, C. (2018). Intercomparison of
757 Univariate and Joint Bias Correction Methods in Changing Climate From a
758 Hydrological Perspective. *Climate*, 6(2), 33. doi:10.3390/cli6020033

759 Seo, S. B., Das Bhowmik, R., Sankarasubramanian, A., Mahinthakumar, G., & Kumar,
760 M. (2019). The role of cross-correlation between precipitation and temperature
761 in basin-scale simulations of hydrologic variables. *Journal of Hydrology*, 570,
762 304-314. doi:10.1016/j.jhydrol.2018.12.076

763 Shen, M., Chen, J., Zhuan, M., Chen, H., Xu, C.-Y., & Xiong, L. (2018). Estimating
764 uncertainty and its temporal variation related to global climate models in
765 quantifying climate change impacts on hydrology. *Journal of Hydrology*, 556,
766 10-24. doi:10.1016/j.jhydrol.2017.11.004

767 Shrestha, R. R., Cannon, A. J., Schnorbus, M. A., & Alford, H. (2019). Climatic
768 Controls on Future Hydrologic Changes in a Subarctic River Basin in Canada.
769 *Journal of Hydrometeorology*. doi:10.1175/jhm-d-18-0262.1

770 Taylor, K. E., Stouffer, R. J., & Meehl, G. A. (2012). An Overview of CMIP5 and the
771 Experiment Design. *Bulletin of the American Meteorological Society*, 93(4),
772 485-498. doi:10.1175/bams-d-11-00094.1

773 Valéry, A., Andréassian, V., & Perrin, C. (2014). ‘As simple as possible but not simpler’:
774 What is useful in a temperature-based snow-accounting routine? Part 2 –
775 Sensitivity analysis of the Cemaneige snow accounting routine on 380
776 catchments. *Journal of Hydrology*, 517, 1176-1187.
777 doi:10.1016/j.jhydrol.2014.04.058

778 Vano, J. A., Das, T., & Lettenmaier, D. P. (2012). Hydrologic Sensitivities of Colorado
779 River Runoff to Changes in Precipitation and Temperature*. *Journal of*
780 *Hydrometeorology*, 13(3), 932-949. doi:10.1175/jhm-d-11-069.1

781 Volosciuk, C., Maraun, D., Vrac, M., & Widmann, M. (2017). A combined statistical
782 bias correction and stochastic downscaling method for precipitation. *Hydrology*
783 *and Earth System Sciences*, 21(3), 1693-1719. doi:10.5194/hess-21-1693-2017

784 Vrac, M., & Friederichs, P. (2015). Multivariate—Intervariable, Spatial, and
785 Temporal—Bias Correction*. *Journal of Climate*, 28(1), 218-237.
786 doi:10.1175/jcli-d-14-00059.1

787 Yang, X., Magnusson, J., Huang, S., Beldring, S., & Xu, C.-Y. (2019). Dependence of
788 regionalization methods on complexity of hydrological models in multiple
789 climate regions. *Journal of Hydrology*, 582: 124357. doi:
790 10.1016/j.jhydrol.2019.124357

791
792
793
794
795
796
797

798 **Tables**

799 Table 1 Koeppen-Geiger climate classification of 2840 watersheds and the basin
800 number of each climate regime

Climate (Basin Number)	Characteristics	Climate (Basin Number)	Characteristics	Climate (Basin Number)	Characteristics
BSk (47)	Arid, Steppe, Cold Arid	Csb (215)	Warm Temperate, Summer Dry, Warm Summer	Dsb (49)	Snow, Summer Dry, Warm Summer
Cfa (981)	Warm Temperate, Fully Humid, Hot Summer	Dfa (350)	Snow, Fully Humid, Hot Summer	Dsc (18)	Snow, Summer Dry, Cool Summer
Cfb (93)	Warm Temperate, Fully Humid, Warm Summer	Dfb (675)	Snow, Fully Humid, Warm Summer	ET (30)	Polar, Polar Tundra
Csa (20)	Warm Temperate, Summer Dry, Hot Summer	Dfc (362)	Snow, Fully Humid, Cool Summer		

801

802 Table 2 The summary of the seven bias correction methods

Name	Type	Description	Citation
Daily bias correction (DBC)	Univariate	Quantile mapping-based, correcting the biases in the cumulative distribution function of each variable	Chen et al., 2013b
Joint bias correction (JBC)	Multivariate	Copula function-based, establishing the copula function for multiple variable first and then correcting one variable conditionally upon the other one	Li et al., 2014
Multivariate bias correction: Pearson version (MBCp)	Multivariate	Shuffle-based, inducing the desired Pearson correlation matrix by iteration algorithm	Cannon, 2016
Multivariate bias correction: Spearman version (MBCr)	Multivariate	Shuffle-based, inducing the desired Spearman correlation matrix by iteratively adjusting the time sequence of simulated variable	Cannon, 2016
Multivariate bias correction: N-dimensional probability density function transform (MBCn)	Multivariate	Rotation-based, inducing the desired multivariate distribution function by iteratively rotation and correction	Cannon, 2017
Two-stage quantile mapping (TSQM)	Multivariate	Shuffle-based, inducing the desired Spearman correlation matrix by distribution-free shuffle algorithm	Guo et al., 2019
Empirical Copula bias correction (ECBC)	Multivariate	Shuffle-based, reproducing the observed correlation matrix by reordering the time sequence of simulated variables to corresponding observations	Vrac & Friederichs, 2015

803

804 Table 3 The ratio (%) that the mean values of RMSE of multivariate methods are
805 smaller than DBC in simulating the 9 streamflow variables for the validation period

	Spring mean flow	Summer mean flow	Autumn mean flow	Winter mean flow	High flow	Low flow	Peak time	Flood begin time	Flood end time	In general
Arid	67	17	67	83	67	67	100	83	83	70
Warm temperate	88	42	67	79	71	50	83	79	79	71
Snow	53	10	67	73	53	57	57	40	77	54
Polar	33	0	33	50	67	33	83	100	100	55
In general	67	27	65	74	59	55	73	65	82	63

806

807 **Figure captions**

808 Fig. 1 The 11 climate regimes of the 2840 watersheds in North America based on
809 Koeppen-Geiger climate classification

810

811 Fig. 2 The Nash-Sutcliffe efficiency for the 2840 watersheds in both calibration and
812 validation periods using GR4J-9 hydrological model

813

814 Fig. 3 The root-mean-square-error of variable means for P, T_{\max} , and T_{\min} for 4 typical
815 months over the 2840 watersheds in the validation period. The x-axis label from left
816 to right is DBC, JBC, MBCp, MBCr, MBCn, TSQM and ECBC, respectively,
817 representing seven bias correction methods. On each box, the central mark indicates
818 the median, and the bottom and top edges of the box indicate the 25th and 75th
819 percentiles, respectively. The whiskers extend to the most extreme data points not
820 considered outliers, and the outliers are plotted individually using the red '+' symbol

821

822 Fig. 4 The spatial distribution of observed and corrected simulated (BCC-CSM1.1 (m)
823 as an example) P- T_{\max} correlation of July for the 2840 watersheds in the validation
824 period. OBS represents P- T_{\max} correlation of reference data, and DBC, JBC, MBCp,
825 MBCr, MBCn, TSQM and ECBC represent the corrected P- T_{\max} correlation by the
826 corresponding bias correction method, respectively

827

828 Fig. 5 The root-mean-square-error for the 2840 watersheds between the observed and
829 corrected P- T_{\max} and P- T_{\min} correlation for 4 typical months in both calibration ((a)
830 and (b)) and validation ((c) and (d)) periods. The x-axis label from left to right is DBC,
831 JBC, MBCp, MBCr, MBCn, TSQM and ECBC, respectively, representing seven bias
832 correction methods. On each box, the central mark indicates the median, and the
833 bottom and top edges of the box indicate the 25th and 75th percentiles, respectively.
834 The whiskers extend to the most extreme data points not considered outliers, and the
835 outliers are plotted individually using the red '+' symbol

836

837 Fig. 6 The spatial distribution of the absolute error in % of winter snowfall proportion
838 between the reference data and the model outputs (including the raw data and
839 corrected data) for the 2840 watersheds in the validation period. RAW represents the
840 result of climate model outputs without bias correction, and DBC, JBC, MBCp,
841 MBCr, MBCn, TSQM and ECBC represent the result of the corresponding bias

842 correction method, respectively

843

844 Fig. 7 The spatial distribution of the absolute relative error (%) of spring daily mean
845 snowmelt between the reference data and the model outputs (including the raw data
846 and corrected data) for the 2840 watersheds in the validation period. RAW represents
847 the result of climate model outputs without bias correction, and DBC, JBC, MBCp,
848 MBCr, MBCn, TSQM and ECBC represent the result of the corresponding bias
849 correction method, respectively

850

851 Fig. 8 The spatial distribution of the daily potential evaporation difference between
852 dry day and wet day (dry days minus wet days) in summer between the reference data
853 and the corrected model outputs for the 2840 watersheds in the validation period.
854 OBS represents the result of reference data, and DBC, JBC, MBCp, MBCr, MBCn,
855 TSQM and ECBC represent the result of the corresponding bias correction method,
856 respectively

857

858 Fig. 9 The Dunnett-t test of root-mean-square-error in simulating winter snowfall
859 proportion, spring daily mean snowmelt and summer wet day evaporation in both
860 calibration and validation periods. The x-axis label represents 11 climate regimes, and
861 the y-axis label represents 6 multivariate bias correction methods. The blue color
862 represents the multivariate method is significantly better than DBC, while the red
863 color represents the multivariate method is significantly worse than DBC, and white
864 color represents there is no significant difference between these two methods. This is
865 also applicable to the Figures hereafter

866

867 Fig. 10 The Dunnett-t test of root-mean-square-error in simulating mean streamflow
868 for 4 seasons in both calibration and validation periods. The x-axis label represents 11
869 climate regimes, and y-axis label represents 6 multivariate bias correction methods

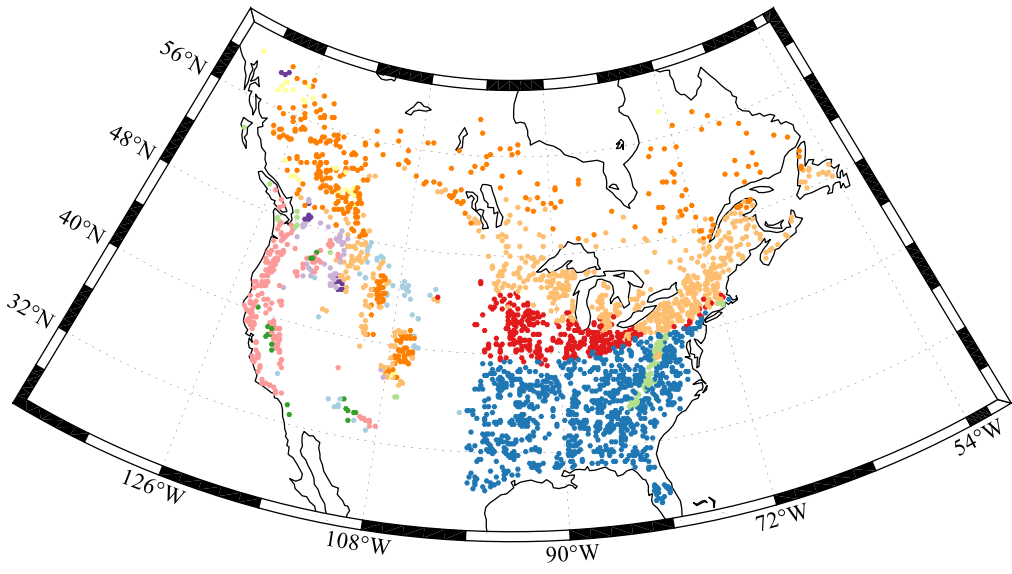
870

871 Fig. 11 The Dunnett-t test of root-mean-square-error in simulating high and low flow
872 in both calibration and validation periods. The x-axis label represents 11 climate
873 regimes, and y-axis label represents 6 multivariate bias correction methods

874

875 Fig. 12 The Dunnett-t test of root-mean-square-error in simulating time variables in
876 both calibration and validation periods. The x-axis label represents 11 climate regimes,
877 and y-axis label represents 6 multivariate bias correction methods

Figure 1.



BSk Cfa Cfb Csa Csb Dfa Dfb Dfc Dsb Dsc ET

Figure 2.

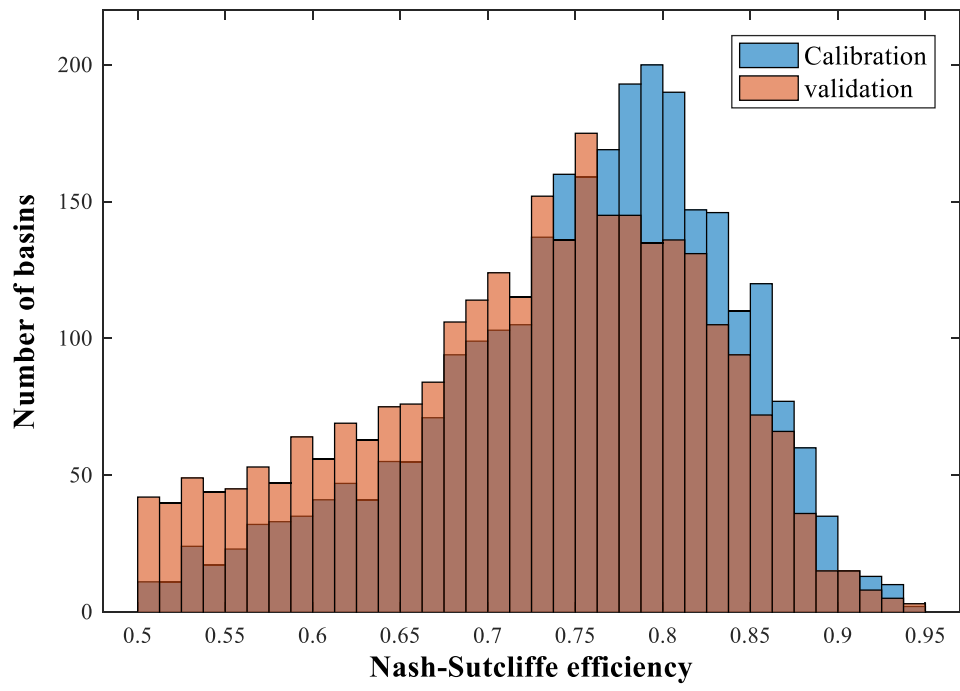


Figure 3.

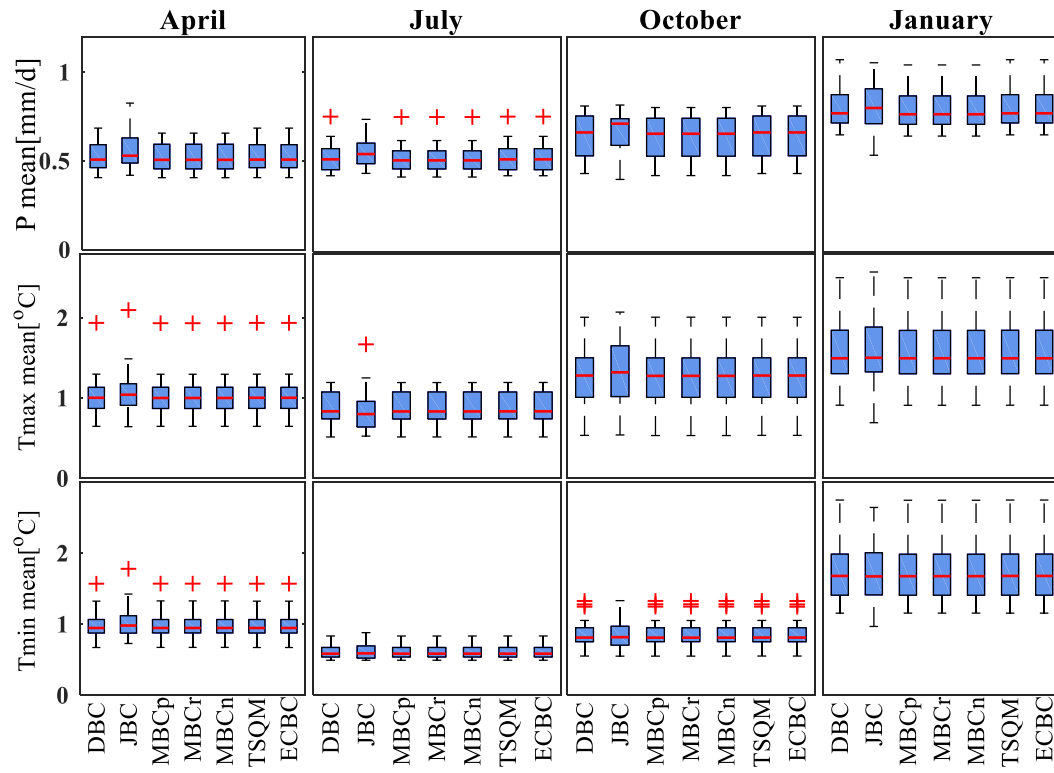


Figure 4.

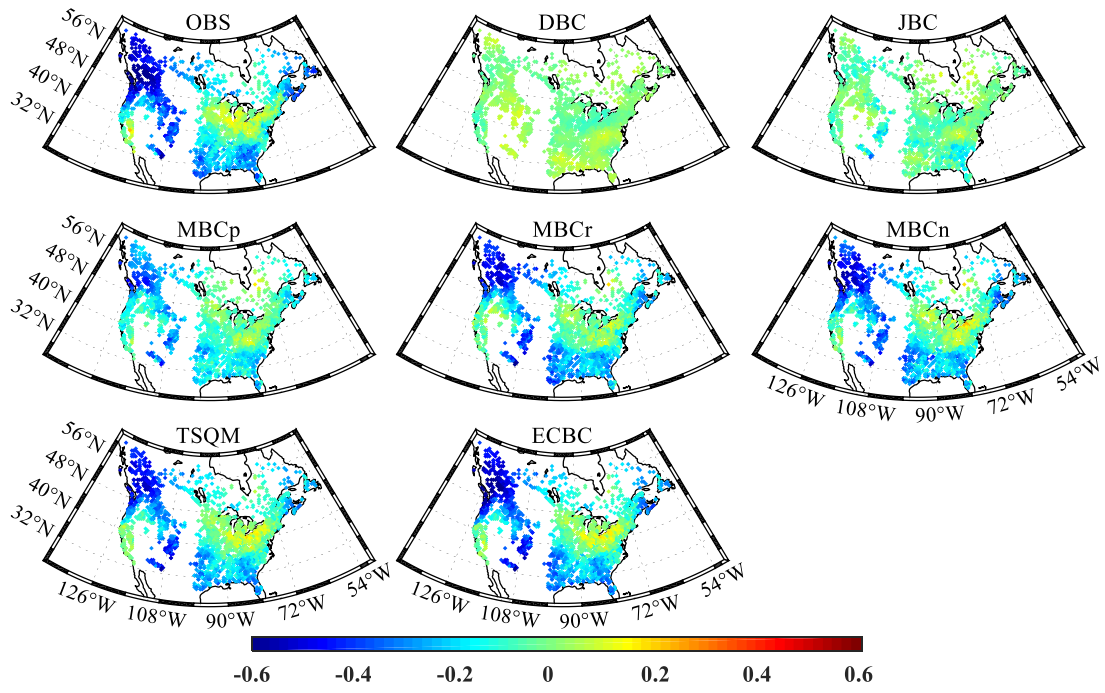


Figure 5.

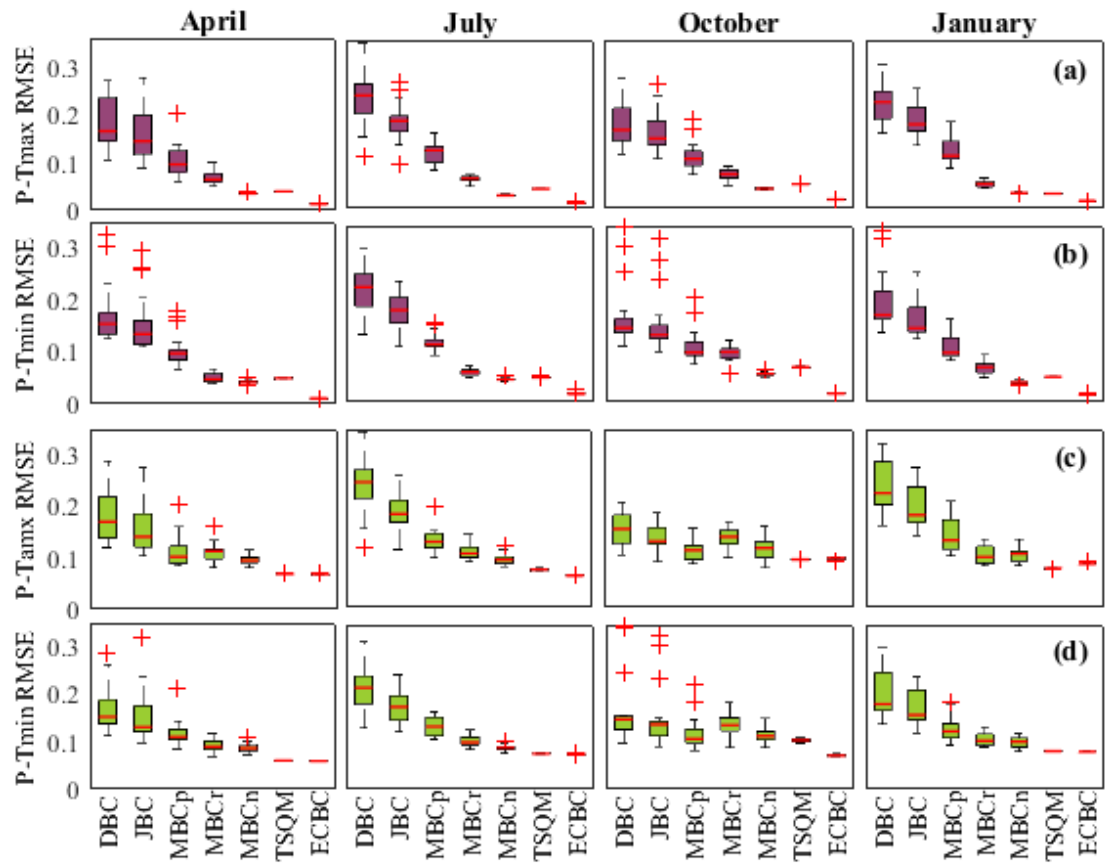


Figure 6.

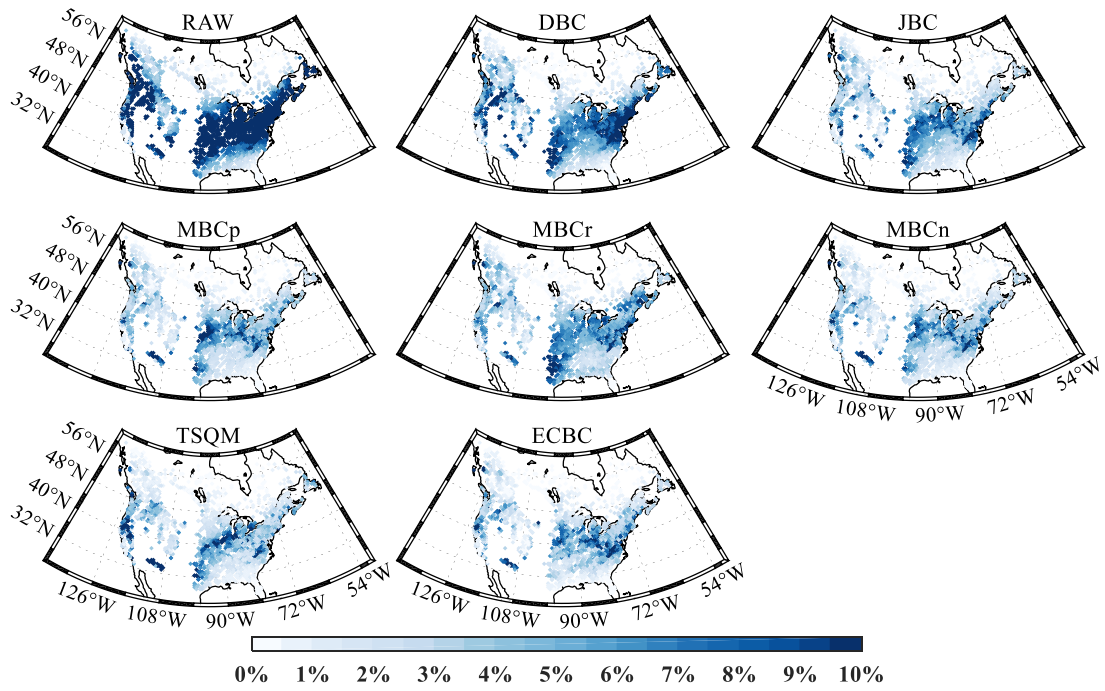


Figure 7.

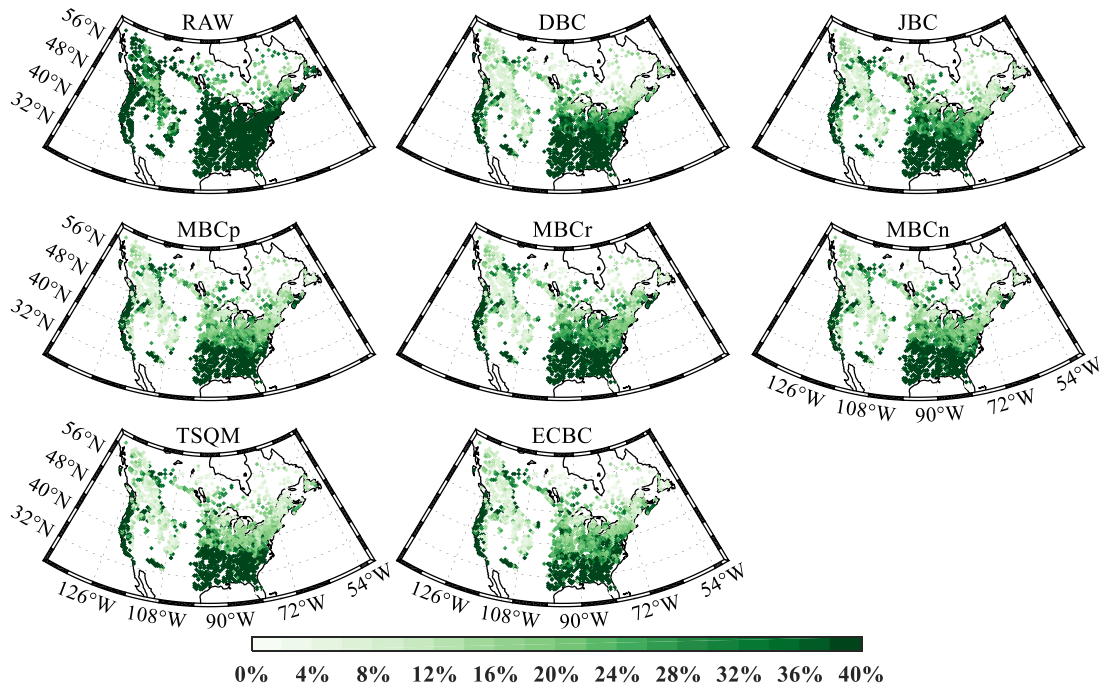


Figure 8.

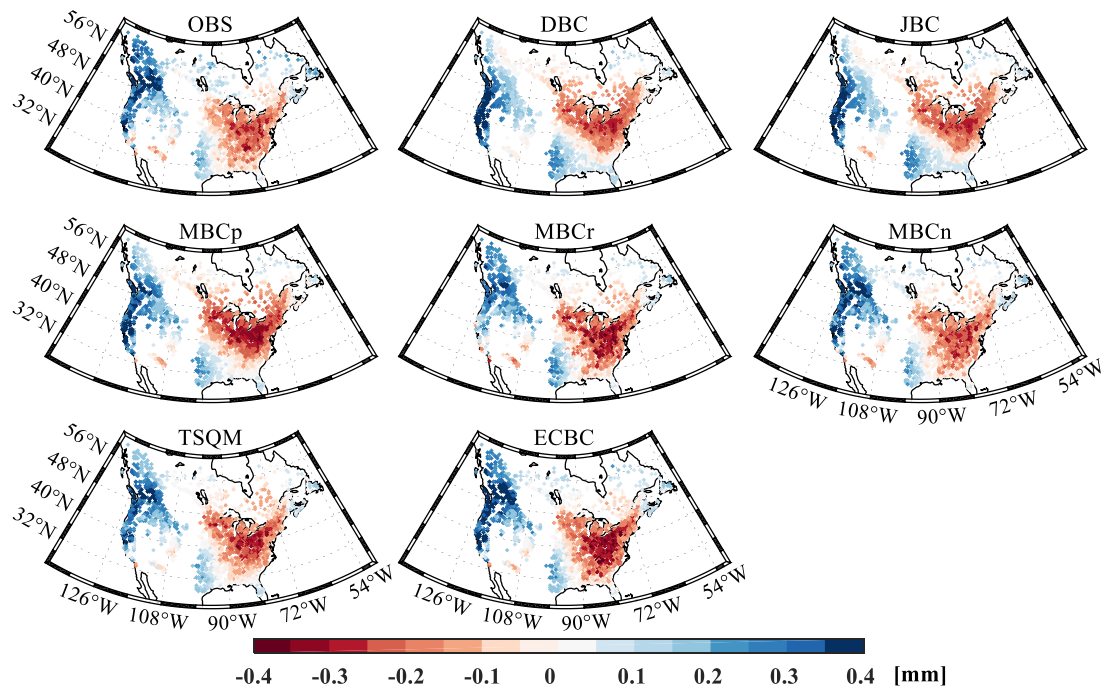


Figure 9.

Figure 10.

Figure 11.

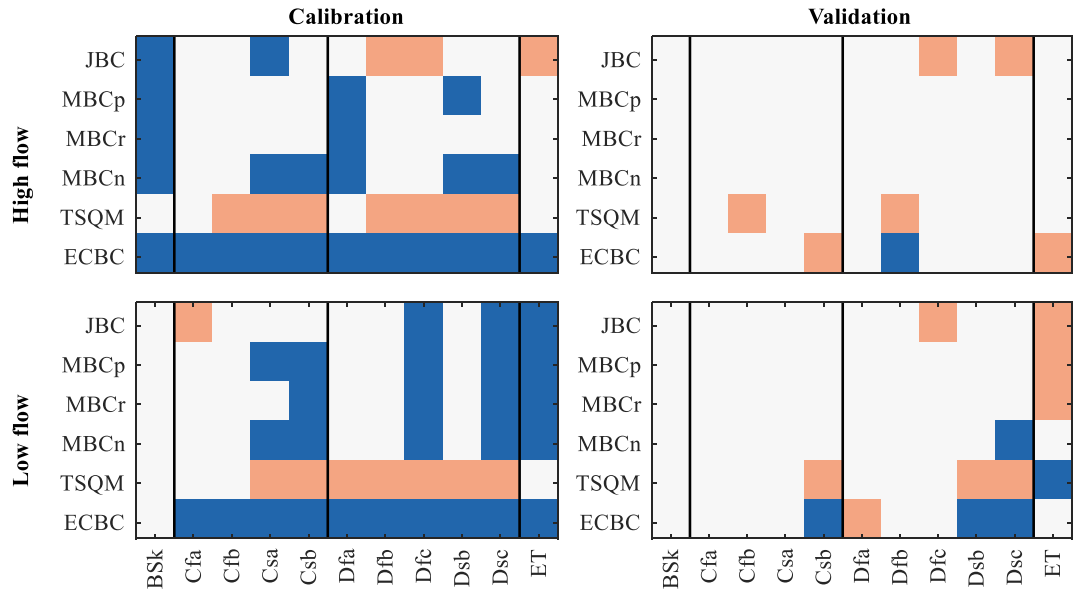


Figure 12.

